Published in final edited form as:
J Comp Neurol. 2011 August 15; 519(12): 2320–2334. doi:10.1002/cne.22618.

Dlx6 Regulates Molecular Properties of the Striatum and Central Nucleus of the Amygdala

Bei Wang[1], **Thomas Lufkin**[2], and **John L. R. Rubenstein**[1,*]

[1]Department of Psychiatry and the Nina Ireland Laboratory of Developmental Neurobiology, University of California San Francisco, San Francisco, California 94158-2324

[2]Genome Institute of Singapore, Singapore 138672

Abstract

We describe here the prenatal telencephalic expression of *Dlx6* RNA and β-galactosidase driven from a mutant *Dlx6* locus. The mutant *Dlx6* allele, which we believe is either a null or severe hypomorph, has an IRES-lacZ-neomycin resistance cassette inserted into the *Dlx6* homeobox coding sequence ($Dlx6^{LacZ}$). We compared expression from the *Dlx6-lacZ* ($Dlx6^{LacZ}$) allele in heterozygotes ($Dlx6^{LacZ/+}$), with the expression of *Dlx1*, *Dlx2*, *Dlx5* and *Dlx6* RNA. Like these wild-type alleles, $Dlx6^{LacZ}$ is expressed in the developing ganglionic eminences, and their derivatives. Unlike the other *Dlx* genes, *Dlx6* and $Dlx6^{LacZ}$ expression is not readily observed in tangentially migrating interneurons. In addition to *Dlx6*'s expression at later stages of differentiation of many basal ganglia nuclei, it shows particularly robust expression in the central nucleus of the amygdala. Histological analysis of *Dlx6* mutants ($Dlx6^{LacZ/LacZ}$) shows that this homeobox transcription factor is required for molecular properties of the striatum, nucleus accumbens, olfactory tubercle, and central nucleus of the amygdala. For instance, we observed reduced of *Golf*, *RXRγ*, and *Tiam2* expression in the striatum, and reduced *Dlx5* expression in the central nucleus of the amygdala. RNA expression array analysis of the E18.5 striatum was useful in identifying the transcription factors that are expressed in this tissue, but did not identify major changes in gene expression in the $Dlx6^{LacZ/LacZ}$ mutant.

INDEXING TERMS

Dlx; striatum; amygdala; mouse; development

There are six known mammalian *Dlx* genes (*Dlx1*, *-2*, *-3*, *-4*, *-5*, and *-6*); they are organized as three bigene pairs: *Dlx1&2*, *Dlx3&4*, and *Dlx5&6*. The *Dlx* genes are expressed in spatially restricted patterns in multiple embryonic tissues in all vertebrates studied (Panganiban and Rubenstein, 2002). Whereas all six known mouse *Dlx* genes are expressed

---

*CORRESPONDENCE TO: John L. R. Rubenstein, Center for Neurobiology and Psychiatry, Department of Psychiatry, Rock Hall, Room RH 284C, UCSF MC 2611, 1550 4th Street, University of California at San Francisco, San Francisco, CA 94158-2324. john.rubenstein@ucsf.edu.
Bei Wang's present address: Neurobiology, Genentech, Inc., 1 DNA Way, South San Francisco, CA 94080.

Additional Supporting Information may be found in the online version of this article.

in the embryonic face and limbs (Qiu et al., 1997; Depew et al., 2005), only *Dlx1*, *-2*, *-5*, and *-6* are expressed in the central nervous system (CNS) (Liu et al., 1997). In mouse, four *Dlx* genes are expressed in the forebrain (*Dlx1*, *-2*, *-5*, and *-6*) and regulate the differentiation and migration of γ-aminobutyric acid (GABA)ergic neurons (Porteus et al., 1994; Qiu et al., 1995; Anderson et al., 1997a, b, 1999a, b, 2001; Marín et al., 2000; Pleasure et al., 2000; Stühmer et al., 2002b; Yun et al., 2002; Long et al., 2003, 2009a, b; Cobos et al., 2005, 2007).

Within the CNS, *Dlx* expression is restricted to the forebrain in two domains. (Bulfone et al., 1993a, b; Anderson et al., 1997a; Liu et al., 1997; Eisenstat et al., 1999). Domain I is diencephalic, and domain II includes most of the subpallial telencephalon. Within the subpallial telencephalon, the *Dlx* genes are expressed in parts of the septum, lateral and medial ganglionic eminences (LGE and MGE, respectively), preoptic area, and centromedial parts of the amygdala (not shown), as well as in pallial interneurons. The expression of the DLX proteins is nearly identical to the expression of the enzymes that synthesize GABA (glutamic acid decarboxylases 1 and 2 [GAD1 and GAD2, previously known as GAD67 and GAD65) (Stühmer et al., 2002a). *Dlx1/2*$^{-/-}$ mutants have reduced GAD1 expression (Long et al., 2007, 2009a, b).

Dlx1, *Dlx2*, *Dlx5*, and *Dlx6* tend to be expressed at different stages of differentiation (Anderson et al., 1997a; Liu et al., 1997; Eisenstat et al., 1999; Long et al., 2009a, b). In general, *Dlx2* is expressed before *Dlx1; Dlx1* precedes *Dlx5*; and *Dlx5* precedes *Dlx6*. The distribution of *Dlx* RNAs and proteins appears to be the same (Eisenstat et al., 1999); DLX6 protein expression has not been assessed. Dlx1 and Dlx2 are co-expressed in a subset of the most immature cells (i.e., cells in the ventricular zone [VZ]) and appear to be co-expressed in the subventricular zone (SVZ). *Dlx5* RNA expression is largely excluded from the VZ, but is strong in the SVZ and postmitotic neurons of the mantle zone (MZ). Finally, *Dlx6* RNA expression is weak in the SVZ and strong in the MZ. These results suggest that different *Dlx* genes are required at different stages of differentiation.

Targeted mutations have been made for *Dlx1*, *Dlx2*, *Dlx1&2*, *Dlx5*, *Dlx6*, and *Dlx5&6*. We believe that each mutation is either a null or severe hypomorph, Except for *Dlx1*$^{-/-}$, each is a lethal mutation causing craniofacial defects that contribute to their demise usually on the day of birth (P0) (Qui et al., 1995, 1997; Depew et al., 1999, 2002, 2005; Jeong et al., 2008). CNS defects are subtle in the *Dlx1*, *Dlx2*, and *Dlx5* single mutants (Qiu et al., 1995, 1997; Long et al., 2003; Cobos et al., 2005). In contrast, *Dlx1&2* double mutants have a severe block in forebrain differentiation and migration associated with increased notch-signaling and increased oligodendrogenesis (Bulfone et al., 1993b, 1998; Anderson et al., 1997a, b; Marín et al., 2000; Pleasure et al., 2000; Yun et al., 2002; Long et al., 2007, 2009a, b; Petryniak et al., 2007). *Dlx5&6* double mutants have ex*encephaly* (Beverdam et al., 2002; Depew et al., 2002) and defects in MGE-derived interneurons (Wang et al., 2010). The observed forebrain phenotypes of *Dlx* single mutants include: *Dlx1*$^{-/-}$, abnormal differentiation and death of dendrite-innervating cortical interneurons (Cobos et al., 2005); *Dlx2*$^{-/-}$, reduction in olfactory bulb tyrosine hydroxylase^{+} interneurons (Qiu et al., 1995); and *Dlx5*$^{-/-}$, reduction in olfactory bulb tyrosine hydroxylase^{+} and GABA^{+} interneurons,

and abnormal parvalbumin interneurons (Levi et al., 2003; Long et al., 2003; Perera et al., 2004; Wang et al., 2010).

Previously, we demonstrated the function of *Dlx6*, alone and in combination with *Dlx5*, during craniofacial development (Depew et al., 2002, 2005; Jeong et al., 2008). Here we describe our analysis of Dlx6 function in the telencephalon. Although histogenesis appears intact, there are molecular defects in the striatum (dorsal and ventral) and the central nucleus of the amygdala.

MATERIALS AND METHODS

Animals

Mice were maintained in standard conditions with food and water ad libitum. All experimental procedures were approved by the Committee on Animal Health and Care at the University of California, San Francisco (UCSF). Mouse colonies were maintained at UCSF, in accordance with National Institutes of Health and UCSF guidelines.

We used the following strains in this study: $Dlx6^{LacZ/+}$ (Jeong et al., 2008), BAC-Dopamine receptor 1-GFP (D1R); BAC-Dopamine-receptor 2-GFP (D2R); and BAC muscarinic receptor M4-GFP (M4R) (http://www.gensat.org/index.html; Lobo et al., 2006). Through the information available to us, the expression patterns of these BAC-GFP strains appeared indistinguishable from the authentic expression patterns of these genes in the striatum, based on our in situ hybridization analyses (Long et al., 2009a and data not shown), the analyses of Lobo et al. (2006), and gene expression results shown at the Allen Institute for Brain Science (http://www.brainmap.org/). However, we did not examine the BAC-GFP transgene expression outside of the striatum and its projections, nor did we perform double labeling with antibody or in situ probes for the authentic genes; therefore we do not wish to imply that their expression is definitely eutopic.

For staging of embryos, midday of the *vaginal* plug was calculated as embryonic day 0.5 (E0.5). Polymerase chain reaction (PCR) genotyping was performed as described (Anderson et al., 1997b; Parras et al., 2004). Because no obvious differences in the phenotypes of $Dlx6^{+/+}$ and $Dlx6^{+/-}$ brains have been detected, they were both used as controls. In the figures, we state explicitly which genotype was used as the control.

To generate the *Dlx6-lacZ* ($Dlx6^{LacZ}$) allele, a 4.3-kb *Spe*I-*Sna*BI genomic fragment spanning *Dlx6* exon 3 (which encodes the homeodomain) was subcloned into the *Spe*I-*Sma*I sites of pBS KS+. Site-directed mutagenesis was performed to engineer a unique *Nru*I site immediately following the 219th amino acid from the N-terminus of the Dlx6 protein (F of the sequence VKIWFQNKRS). Flanking genomic sequences were added between the unique 5′ *Xho*I site (5.8-kb 5′ homology arm) and the 3′ *Not*I site (3.5-kb 3′ homology arm). The reporter cassette IRES-lacZ-PGKneo (Robledo et al., 2002) was cloned into the unique *Nru*I site to generate the final targeting construct. The $Dlx6^{LacZ}$ allele therefore interrupts the Dlx6 protein immediately following the amino acid F, within the homeodomain sequence. This insertion prevents translation of one-third of the homeodomain and the entire C-terminal domain, including the nuclear localization signal

(amino acids 220–228); thus, this allele is likely to be null, although, because no effective anti-DLX6 antibody is available, a precise analysis of the protein products from this allele has not been performed.

RNA preparation and gene expression array analysis

We dissected the rostral striatum from Vibratome sections of E18.5 wild type and *Dlx6*$^{LacZ/LacZ}$ brains. RNA was purified and shipped to the NINDS/NIMH Microarray Consortium (TGEN; http://arrayconsortium.tgen.org/) where biotin-labeled cRNA hybridization probes were generated by using Affymetrix's GeneChip IVT Labeling Kit (Santa Clara, CA), which simultaneously performs in vitro transcription (a linear ~20–60-fold amplification) and biotin labeling. The samples were hybridized to the Affymetrix Mouse Genome 430 2.0 array. TGEN uses GeneChip Operating Software (GCOS) to scan the arrays and to perform a statistical algorithm that determines the signal intensity of each gene (see Cobos et al., 2007; Long et al., 2009a, b for details; the hybridization results of these arrays are available at http://arrayconsortium.tgen.org).

Tissue preparation, in situ hybridization, and immunohistochemistry

We compared gene expression by either in situ hybridization or immunohistochemistry in wild type and *Dlx6*$^{LacZ/LacZ}$ mutants. Preparation of sectioned embryos, immunohistochemistry, and in situ hybridization were performed with antibodies and digoxigenin riboprobes on 20-μm frozen sections cut on a cryostat by using methods described in Wang et al. (2009) and Long et al. (2009a, b). The antibodies and plasmids used in this analysis are described in Tables 1 and 2. The specificity of the antibodies is as follows:

1. **Calbindin (CB)**. The calbindin D28k antibody was characterized by Western blot. The antibody reacts specifically to a single band at 28 kDa on Western blot of rat hippocampal cells (Kim et al., 2006). Immunostaining of mouse embryo brain sections produces a specific staining pattern of calbindin-positive neurons identical to that published previously (in the mouse brain atlas of Jacobowitz and Abbott, 1998).

2. **Calretinin (CR)**. The calretinin antibody was characterized as described (Schwaller et al., 1993), and is also described on the antibody database of this journal (Fischer et al., 2007). Briefly, this antibody detects a single band corresponding to the size of calretinin on Western blot of brain homogenates from human, monkey, rat, and mouse. It labels a subpopulation of neurons in the wild-type mouse brain sections, but does not stain the brain of calretinin knock-out mice (Schiffmann et al., 1999).

3. **CTIP2**. The anti-CTIP2 monoclonal antibody 25B6 was characterized as described (Senawong et al., 2003). On immunoblot prepared from nuclear extract from Jurkat cells immunoprecipitated with anti-Sir2 antibody, the antibody detects two bands corresponding to two isoforms of CTIP2 at about 120 kDa. Immunohistochemistry in mouse brain sections shows expression patterns that are indistinguishable from the RNA expression patterns (Zhao et al., 2008).

4. **DARPP-32**. This antibody was characterized by the manufacturer with Western blot on Jurkat lysate, which shows that the antibody detects a single band at 23 kDa corresponding to DARPP-32. Imunohistochemistry shows patterns of cellular morphology and distribution in the cortex and striatum consistent with published reports (Pardo et al., 2006).

5. **FoxP1**. The FoxP1antibody was characterized by Western blot on Jurkat nuclear extract. According to the manufacturer, this antibody detects the largest three of four isoforms that have been shown to migrate at approximately 97, 68, and 50 kDa. Immunostaining shows a pattern of cellular morphology and distribution in the mouse brain consistent with published reports (Regad et al., 2009).

6. **GFP**. According to the manufacturer, this anti-green fluorescent protein (GFP) antibody detects a band on Western blot corresponding to the size of GFP. No staining was detected on brain sections from wild-type mice.

7. **PH3**. The antibody to phospho-histone H3 was characterized by the manufacturer with Western blot on acid extracts of colcemid-treated HeLa cells. It shows that the antibody detects a single band at 17 kDa corresponding to phospho-histone H3. Immunohistochemistry shows that the antibody labels mitotic cells.

X-gal histochemistry

Brains used for X-gal staining were fixed in 4% paraformaldehyde for 1 hour (for E12.5) or 2 hours (for E15.5 and E18.5) at 4°C, and then sectioned with a cryostat at 20 μm. Sections were rehydrated in 1X phosphate-buffered saline (PBS), incubated in a solution of 10 mM Tris-HCl, pH 7.3, 0.005% Na deoxycholate, 0.01% Nonidet P40, 5 mM K_4FeCN_6, 5 mM K_3FeCN_6, 2 mM $MgCl_2$, and 0.8 mg/ml X-gal for 24 hours to reveal cells expressing LacZ. Samples were washed twice with PBS, dehydrated in an ethanol series (50%, 70%, 90%, 100%) and xylene for 30 seconds each, and then mounted with Aqua poly-mount and a coverslip (Polysciences, Warrington, PA, #18606).

Microscopy

Images of in situ hybridization and immunohistochemistry results were captured by using a Zeiss AxioCam MR (Thornwood, NY) and saved as TIFF files. The images were then processed in Adobe Photoshop CS3 (San Jose, CA). Image backgrounds of the mutants and controls were adjusted to the same level.

Quantitative analysis of LacZ expression in the striatum and gene expression changes in central nucleus of the amygdala (CeA)

The density of LacZ expression in the striatum of *Dlx6*$^{LacZ/+}$ and *Dlx6*$^{LacZ/LacZ}$ mice, and gene expression signals in the CeA of wild-type and *Dlx6*$^{LacZ/LacZ}$ mice were quantified by using ImageJ. The images were imported into ImageJ, and regions of interest (ROIs) were drawn with the polygon selection tool. For each image, a ROI was drawn in the CeA region and another ROI in an area devoid of specific signals to measure background signal. The average brightness value in each ROI was then measured by the Histogram function. LacZ intensity in the striatum (Str) and in situ signal intensity in CeA were calculated by the

following equations: I_{Str} equals; $B_{background} - B_{Str}$ and I_{CEA} equals; $B_{background} - B_{CEA}$, respectively. I signifies signal intensity, and B signifies brightness. Because stronger (LacZ or in situ) signals result in smaller brightness values, $B_{background} - B_{Str}$ will yield a positive value. In each pair of *Dlx6*$^{LacZ/+}$ and *Dlx6*$^{LacZ/LacZ}$ or wild-type and *Dlx6*$^{LacZ/LacZ}$ images, the ROIs have the same shape and size. The graph of gene expression signal intensity was then generated in Microsoft Excel.

RESULTS

Dlx6 and Dlx6^{LacZ} basal ganglia expression at E12.5, E15.5, and E18.5 in Dlx6$^{LacZ/+}$ and Dlx6$^{LacZ/LacZ}$

Previous studies have briefly described *Dlx6* expression in the developing basal ganglia (Anderson et al., 1997b; Liu et al., 1997; Long et al., 2009a, b). Here, we examined in detail the expression of *Dlx6* RNA by using in situ hybridization and β-galactosidase expression from the *Dlx6*^{LacZ} allele. (This allele appears to be a null, or at least a severe hypomorph; see Materials and Methods, and Jeong et al., 2008).

The level of *Dlx6* RNA expression was low compared with other transcription factors in the E15.5 ganglionic eminences (Long et al., 2009a, b) or E18.5 striatum (Supplementary Table 1). For instance, at E15.5 *Dlx6* expression in the MGE was roughly 20-fold less than *Dlx1* and roughly 4-fold less than *Dlx5* (see Table 1 in Long et al., 2009a). In the E18.5 striatum *Dlx6* expression was roughly 10-fold less than *Dlx1* and roughly 5-fold less than *Dlx5*. The relatively low level of *Dlx6* RNA limited the sensitivity of the in situ RNA hybridization array analysis. Nevertheless, we did not detect an obvious difference between the *Dlx6* RNA and βgalactosidase expression (Figs. 1, 2). Therefore, we concentrated our description on the β-galactosidase expression from the *Dlx6*^{LacZ} allele because it was easier to detect and it gave better cellular resolution.

Dlx6 expression at E12.5, E15.5, and E18.5, like other Dlx genes, encompasses most subpallial regions (Eisenstat et al., 1999; Stühmer et al., 2002b). However, unlike *Dlx1* and *Dlx2*, *Dlx6* expression was restricted to the SVZ of the septum, LGE, MGE, POA, and CGE, and mantle of the septum, nucleus accumbens (NAc), striatum (Str), and central nucleus of the amygdala (CeA).

Dlx6 expression was conspicuously low in the olfactory bulb (and the SVZ of the dLGE), olfactory tubercle (OT), and preoptic area, and was not detectable in the ventral pallidum, globus pallidus, medial amygdale, and cortical/hippocampal interneurons. The low expression in these regions contrasts with the expression of its closest paralogue, *Dlx1* (Fig. 8C; Cobos et al., 2005; Long et al., 2007). This suggests that Dlx1 function is more important than Dlx6 in the olfactory bulb, olfactory tubercle, pre-optic area, ventral pallidum, globus pallidus, medial amygdale, and cortical/hippocampal interneurons, whereas *Dlx6* may be more important than *Dlx1* in the development of the CeA. *Dlx5* and *Dlx6* share similar patterns of expression, although *Dlx5* expression was higher in the SVZ of the LGE and higher in the OT and ventral striatum/NAc (Figs. 3A, B, 4A, B). *Dlx6*, and its antisense transcript (Liu et al., 1997; Faedo et al., 2004; Feng et al., 2006; Bond et al., 2009), showed inverse expression gradients in the striatum and OT, and complementary pallial/subpallial

expression (Fig. 3B, C). The function of the *Dlx6* antisense transcript is uncertain, but it could regulate expression of *Dlx6*.

Next we assessed the effect of the $Dlx6^{LacZ/LacZ}$ mutation on the expression of *Dlx6*. Generation of the *Dlx6* mutation involved an insertion of the LacZ gene into exon 3 (see Materials and Methods and Robledo et al., 2002; Jeong et al., 2008). Thus, we could study the effect of the mutation on the expression of both the 5′ end of the *Dlx6* gene (exons 1 and 2) and the LacZ gene. Expression of both the truncated *Dlx6* RNA (exons 1 and 2) and β-galactosidase was increased in most regions of the subpallium in $Dlx6^{LacZ/LacZ}$ compared with $Dlx6^{LacZ/+}$ (Figs. 1, 2). Within the E18.5 striatum (Str), the distribution of LacZ expression was non-uniform; it appeared patchy (lower expression in the patch-like domains) and showed a gradient (high lateral-low medial); this distribution of LacZ expression was disrupted in the $Dlx6^{LacZ/LacZ}$ mutant. Furthermore, the mutant showed much higher, and perhaps ectopic, expression in the OT and core of nucleus accumbens (NAcC). The increase in β-galactosidase in the $Dlx6^{LacZ/LacZ}$ mutant in the striatum and central nucleus of the amygdala (CeA) was roughly twofold more than in the $Dlx6^{LacZ/+}$ heterozygotes (Supplementary Fig. 5).

Only three structures in the mutant showed reduced *Dlx6* RNA expression: the SVZ of the LGE and septum, and the mantle zone of the CeA (Figs. 1D, D′, H, H′, L, L′ P, P′, 3B, B′, 7B, B′, 8B, B′). Despite the reduced RNA expression, LacZ expression remained strong in the CEA (Fig. 2). This suggests that the CeA is produced, but may have a molecular defect. Below we describe molecular defects in the NAcC, Str, OT, and CeA in the $Dlx6^{LacZ/LacZ}$ mutant.

Gene expression array analysis of the E18.5 $Dlx6^{LacZ/LacZ}$ striatum

To obtain an unbiased identification of gene dysregulation in the $Dlx6^{LacZ/LacZ}$ mutants, we performed gene expression array analysis in the E18.5 striatum. We dissected the rostral striatum from Vibratome sections of wild-type and $Dlx6^{LacZ/LacZ}$ brains. RNA was prepared and used for hybridization to Affymetrix Mouse Genome 430 2.0 arrays. From these data we generated a list of transcription factors that are expressed in the wild-type striatum, and arranged the list as a function of their relative expression levels (Supplementary Table 1). We found that *Dlx6* was expressed at much lower levels than most other transcription factors. For instance *FoxP1*, *FoxG1*, and *Isl1* were expressed at 32-, 24-, and 15-fold higher levels, respectively. Unfortunately, comparison of wild type and $Dlx6^{LacZ/LacZ}$ mutants did not reveal any robust changes in gene expression, including genes studied by in situ hybridization (Supplementary Table 2); all of the data are at http://arrayconsortium.tgen.org, even for genes showing expression changes found by the histochemical analyses described below. We believe that this is because the phenotype is subtle, and that many of the gene expression changes are alterations in RNA distributions rather than frank loss or gain of expression.

Changes in expression of LGE and striatal markers at E15.5 and E18.5 in $Dlx6^{LacZ/LacZ}$

β-Galactosidase expression in $Dlx6^{LacZ/LacZ}$ telencephalon was disrupted in the striatum (changes in its gradient and patchy distribution), and showed much higher (perhaps ectopic)

expression in the OT and NAcC (Fig. 2). We compared the expression of ~40 genes by either in situ hybridization or immunohistochemistry in wild type and *Dlx6*$^{LacZ/LacZ}$ mutants; most of these markers were chosen because their expression was altered in the basal ganglia of the *Dlx1/2*$^{-/-}$ mutants (Long et al., 2009a; Long et al., 2009b). Below we describe abnormalities in the expression for several of these genes (Figs. 1–4; Supplementary Figs. 1, 2).

At E15.5, *Dlx5* expression was reduced in the mutant OT (Fig. 3A, A′). Furthermore, the relative levels of *Dlx5* expression in the mutant LGE SVZ and striatum were similar (also seen in the septum), unlike in the wild type. At E18.5, these phenotypes were not detected (Fig. 4A, A′). Antisense *Dlx6* expression at E15.5 showed a subtle increase throughout its expression domain (Fig. 3C, C′); at E18.5 its expression appeared increased throughout the striatum and septum (not shown). Reduced striatal expression was noted for *Golf*, *RXR*γ, and *Tiam2* at E15.5 and E18.5 (Figs. 3D, D′, G, G′, H, H′, 4D, D′, E, E′, H. H′). Increased striatal expression was noted for *Ikaros* at E15.5 (Fig. 3E, E′); at E18.5 the increased expression became even more prominent in neurons adjacent to the SVZ (arrow; Fig. 4C, C′). Preprotachykinin (*PPT*) expression was lost in scattered cells in the region of the OT at E15.5 (arrow; Fig. 3F, F′); at E18.5, the patchy striatal *PPT* expression was greatly reduced, especially along the outer margin of the striatum (arrow; Fig. 4G, G′); *Tiam2* also lost expression in this region (arrow; Fig. 4E,'E). Likewise, DARPP-32 striatal expression in patch-like domains was less distinct (Fig. 4I, I′). The gradient of *Pbx3* striatal expression was altered, and its expression appeared increased in the NAc (arrow; Fig. 4F, F′).

Next, to study the effect of the *Dlx6* mutation on axon projections from the striatum, we introduced three different BAC-GFP transgenes into the *Dlx6*$^{+/-}$ background: BAC-Dopamine receptor 1-GFP (D1R); BAC-Dopamine-receptor 2-GFP (D2R); and BAC muscarinic receptor M4-GFP (M4R) (http://www.gensat.org/index.html; Lobo et al., 2006). D1R and D2R are preferentially expressed in the striatal neurons that project in the direct and indirect pathways, respectively, whereas M4R is robustly expressed in both (Lobo et al., 2006). For each transgene, we generated mice that were *Dlx6*$^{-/-}$; *BAC-GFP*$^{+/-}$, and then studied GFP expression at E18.5 (Figs. 5, 6; Supplementary Figs. 1, 2). For each of these transgenes, we did not observe major changes in expression in the striatum, nor an obvious defect in striatal axonal projects. However, in the *Dlx6* mutant the M4R-GFP line showed increased GFP^{+} staining in the NAc (Fig. 5A, A′, B, B′; similar to *Pbx3* in Fig. 4F, F′), and may have an abnormal accumulation of axons leaving the striatum (Fig. 5D, D′).

Finally, we followed the trajectory of the M4R-GFP axons to the midbrain and their target zone in the substantia nigra (Fig. 6). We compared expression of GFP, with glutamic acid decarboyxylase 1 (GAD1; marker of pars reticulata) and tyrosine hydroxylase (TH; marker of pars compacta). We did not observe a clear defect in the ability of the GFP^{+} striatal axons to project to the substantia nigra (Fig. 6).

Changes in expression of central nucleus of the amygdala (CeA) markers at E15.5 and E18.5 in wild type and Dlx6$^{LacZ/LacZ}$

In wild-type mice *Dlx5* and *Dlx6* were expressed in the CeA (Figs. 1H, P, 7A, B, 8A, B), whereas *Dlx1* was expressed in the medial amygdala (MeA), bed nucleus stria terminalis

intraamygdaloid (STIA), basomedial (BM), and corticoid (Co) nuclei, as well as in scattered cells of the intercalated nuclei (ITC) and within the pallial amygdala (lateral and basolateral) (Fig. 8C). In the *Dlx6*$^{LacZ/LacZ}$ mutant, *Dlx1* expression may have decreased in the STIA, BM, and Co (Fig. 8C′). *Dlx2* expression in the amygdala was difficult to detect (data not shown).

Dlx6 RNA expression in *Dlx6*$^{LacZ/LacZ}$ mutant showed a conspicuous loss of expression in the central nucleus of the amygdala (CeA) at E15.5 and E18.5 (Figs. 1H, H′, P, P′, 7B, B′, 8B, B′; Supplementary Fig. 4). Thus, we examined the CeA in greater detail by using markers we found that label the CeA, or nearby subpallial components of the amygdala. Like *Dlx6*, *Dlx5* RNA was strongly decreased in the CeA at E15.5 and E18.5 (Figs. 7A, A′, 8A, A′; Supplementary Fig. 4). Reduced expression in the region of the CeA was also detected for *Golf* (arrow; Figs. 7C, C′, 8D, D′; Supplementary Fig. 4) and *Pbx3* (Fig. 7D, D′). *PPT* expression in scattered cells in the CeA was reduced (arrow; Figs. 7E, E′, 8F, F′), as was its expression in the caudoventral striatum (Figs. 7E, E′, 8F, F′).

DISCUSSION

Dlx6 expression: comparison with Dlx1, Dlx2, and Dlx5: overlapping and unique features

The *Dlx6*$^{LacZ/LacZ}$ mutant dies the day of birth with conspicuous craniofacial defects (Jeong et al., 2008). Although its forebrain shows no obvious morphological phenotypes, it does exhibit gene expression abnormalities in striatal and amygdaloid structures. The lack of severe forebrain defects probably reflects compensatory functions of Dlx1, Dlx2, and Dlx5 (Anderson et al., 1997a, b; Depew et al., 2002; Jeong et al., 2008). For instance, although the forebrain of *Dlx1* mutants appears normal, subsets of its cortical and hippocampal neurons have molecular and functional defects that only appear postnatally (Cobos et al., 2005).

Dlx5/6$^{-/-}$ mutants have been generated (Beverdam et al., 2002; Robledo et al., 2002), but their forebrains are difficult to study because of exencephaly (Depew et al., 2002). Nevertheless, we have obtained evidence that *Dlx5/6*$^{-/-}$ mutants have defects in the migration and differentiation (based on transplantation of mutant cells into a wild-type cortex) of MGE-derived interneurons (Wang et al., 2010). We did not observe evidence of LGE molecular defects at E15.5; analysis of their striatal development was not possible due to the abnormal morphology of this region. Generation of a *Dlx5&6* conditional mutant will be important in establishing the function of Dlx5&6 in the developing and postnatal brain.

The low level of *Dlx6* RNA expression (Supplementary Table 1) may also contribute to lack of robust forebrain phenotypes in the *Dlx6*$^{LacZ/LacZ}$ mutants. At E15.5 *Dlx6* expression in the MGE was nearly 20-fold less than *Dlx1* and roughly 4-fold less than *Dlx5* (see Table 1 in Long et al., 2009a). In the E18.5 striatum *Dlx6* expression was about 10-fold less than *Dlx1* and roughly 5-fold less than *Dlx5* (Supplementary Table 1).

Dlx6 expression was restricted to the SVZ of the septum, LGE, MGE, POA, and CGE, and mantle of the septum, nucleus accumbens (NAc), striatum (Str), and central nucleus of the amygdala (CeA) (Figs. 1, 3, 4, 7, 8). Future studies are needed to carefully describe *Dlx6* expression in the diencephalon, where it is prominent in *Dlx*$^{+}$ zones of the prethalamus

(reticular nucleus, zona incerta), anterior hypothalamus, and dorsomedial, suprachiasmatic, and arcuate nuclei (Puelles and Rubenstein, 2003; Yee et al., 2009).

Dlx6 expression was conspicuously low in the olfactory bulb (and the SVZ of the dLGE), olfactory tubercle (OT), and preoptic area, and was not detectable in the ventral pallidum, globus pallidus, medial amygdale, and cortical/hippocampal interneurons. The low expression in these regions contrasts with the moderate/high expression of its closest paralogue, *Dlx1*, in these regions (Fig. 8C; Cobos et al., 2005). Furthermore, the low *Dlx6* expression in interneurons of the olfactory bulb, cortex, and hippocampus contrasts with expression and function of *Dlx1*, *Dlx2*, and *Dlx5* in these cells (Figs. 1, 3, 4, 7, 8; Long et al., 2003, 2007; Cobos et al., 2005; Wang et al., 2010). Thus, we suggest that $Dlx6^{-/-}$ mutants may primarily have molecular and functional defects in forebrain neurons/regions where its expression has minimal overlap with the other *Dlx* genes. However, functional analysis of $Dlx6^{-/-}$ neurons will probably require study of postnatal mutants, and thus necessitate the generation of a *Dlx6* condition allele.

$Dlx6^{LacZ/LacZ}$ mutants show molecular defects in the ventral striatum, dorsal striatum, and central nucleus of the amygdala

Gene expression defects were detected in $Dlx6^{LacZ/LacZ}$ mutants in the SE, NAcC, Str, OT, and CeA. The OT and NAcC normally express low levels of *Dlx6* (compared with the dorsal striatum; Figs. 1, 3, 4); $Dlx6^{LacZ/LacZ}$ mutants showed increased *Dlx6* and LacZ transcripts in the OT and NAcC (Figs. 1, 2). In addition, these regions had increased expression of *Pbx3* (Fig. 4F, F′). These molecular changes in the ventral striatum (OT and NAcC) in the $Dlx6^{LacZ/LacZ}$ mutant provide evidence that *Dlx6* regulates the development of this region.

Molecular defects in the Str and SE appear in their SVZ, which have reduced *Dlx6* expression (Fig. 3B, B′), suggesting that secondary progenitors may be abnormal. However, we did not detect obvious changes in proliferation based on phosphohistone-3 staining (Supplementary Fig. 3). Striatal mantle defects in the $Dlx6^{LacZ/LacZ}$ mutants included reduced expression of several genes that are downregulated in $Dlx1/2^{-/-}$ mutants (Long et al., 2009a, b): *Golf*, *PPT*, *RXRγ*, and *Tiam2* (Figs. 3, 4). These striatal defects included reduced expression of DARPP-32 and *PPT* in patchy domains (Fig. 4), and alterations in the gradients of expression of *Ikaros* and *Pbx3* (Fig. 4). Therefore, we hypothesize that loss of *Dlx6* expression in the $Dlx1/2^{-/-}$ mutants contributes to their LGE/striatal differentiation defects. Further work is needed to definitively establish whether these molecular defects are indicative of alterations in striatal patch (striosomal) development in the $Dlx6^{LacZ/LacZ}$ mutant..

Analysis of striatal projections to the globus pallidus and substantia nigra failed to identify a clear phenotype in the $Dlx6^{LacZ/LacZ}$ mutant (Figs. 5, 6; Supplementary Figs. 1, 2). However, some of these axons appeared abnormal where they exit the telencephalon into the diencephalon (Fig. 5D, D′). Even so, striatal axons expressing M4R reach the substantia nigra (Fig. 6). In sum, striatal molecular architecture was disrupted in the absence of *Dlx6*.

Perhaps the most surprising result of this study was the differential expression of *Dlx1* versus *Dlx5&6* in the amygdala. Whereas *Dlx5* and *Dlx6* were expressed in the CeA, *Dlx1*

was expressed in the medial amygdala (MeA), in other subpallial amygdala nuclei, and in pallial amygdala interneurons (Fig. 8A–C). *Dlx2* expression was difficult to detect in these regions (data not shown).

The *Dlx6*$^{LacZ/LacZ}$ mutant showed greatly reduced expression of *Dlx5* and *Dlx6* RNA in the CeA at E15.5 and E18.5 (Figs. 1H, H′, 7A, A′, B, B′, 8A, A′, B, B′; Supplementary Fig. 4). LacZ expression from the *Dlx6* locus was maintained in the region of the CeA (Fig. 2), supporting the hypothesis that the CeA was present. Thus, we suggest that the CeA is formed in the *Dlx6*$^{LacZ/LacZ}$ mutant, but it has molecular defects. This model is further supported by subtle reduction in the expression of *Golf*, *Pbx3*, *PPT*, and *Six3* (Figs. 7C, C′, D, D′, E, E′, 8D, D′, E, E′, F, F′). These results raise the possibility that *Dlx5* and *Dlx6* are important regulators of CeA development and function, and therefore alterations in Dlx5 and Dlx6 function will affect behaviors linked to the CeA (e.g., anxiety and fear). In this regard, it is interesting that mice with reduced *Dlx1* dosage (*Dlx1*$^{-/-}$ and *Dlx1*$^{+/-}$ mutants) have reduced fear conditioning (Mao et al., 2009). Therefore, distinct members of the *Dlx* family may have important roles in regulating amygdala development and function: *Dlx5* and *Dlx6* in the CeA, and *Dlx1* in the MeA, in other subpallial amygdala nuclei, and in pallial amygdala interneurons.

Supplementary Material

Refer to Web version on PubMed Central for supplementary material.

Acknowledgments

Grant sponsor: Nina Ireland, Larry L. Hillblom Foundation (to J.L.R.R.); National Institute of Mental Health; Grant number: NIMH RO1 MH49428-01; Grant number: NIMH R37 MH049428-16A1; Grant number: K05 MH065670 (to J.L.R.R.); Grant sponsor: National Alliance for Research on Schizophrenia and Depression Young Investigator Award (to B.W.).

We thank Susan Yu for her help in manuscript preparation.

LITERATURE CITED

Anderson S, Mione M, Yun K, Rubenstein JL. Differential origins of neocortical projection and local circuit neurons: role of Dlx genes in neocortical interneuronogenesis. Cereb Cortex. 1999; 9:646–654. [PubMed: 10498283]

Anderson SA, Eisenstat DD, Shi L, Rubenstein JL. Interneuron migration from basal forebrain to neocortex: dependence on Dlx genes. Science. 1997a; 278:474–476. [PubMed: 9334308]

Anderson SA, Qiu M, Bulfone A, Eisenstat DD, Meneses J, Pedersen R, Rubenstein JL. Mutations of the homeobox genes Dlx-1 and Dlx-2 disrupt the striatal sub-ventricular zone and differentiation of late born striatal neurons. Neuron. 1997b; 19:27–37. [PubMed: 9247261]

Anderson SA, Marín O, Horn C, Jennings K, Rubenstein JL. Distinct cortical migrations from the medial and lateral ganglionic eminences. Development. 2001; 128:353–363. [PubMed: 11152634]

Beverdam A, Merlo GR, Paleari L, Mantero S, Genova F, Barbieri O, Janvier P, Levi G. Jaw transformation with gain of symmetry after Dlx5/Dlx6 inactivation: mirror of the past? Genesis. 2002; 34:221–227. [PubMed: 12434331]

Bond AM, Vangompel MJ, Sametsky EA, Clark MF, Savage JC, Disterhoft JF, Kohtz JD. Balanced gene regulation by an embryonic brain ncRNA is critical for adult hippocampal GABA circuitry. Nat Neurosci. 2009; 12:1020–1027. [PubMed: 19620975]

Bulfone A, Gattuso C, Marchitiello A, Pardini C, Boncinelli E, Borsani G, Banfi S, Ballabio A. The embryonic expression pattern of 40 murine cDNAs homologous to *Drosophila* mutant genes (Dres): a comparative and topographic approach to predict gene function. Hum Mol Genet. 1998; 7:1997–2006. [PubMed: 9817915]

Bulfone A, Kim HJ, Puelles L, Porteus MH, Grippo JF, Rubenstein JL. The mouse Dlx-2 (Tes-1) gene is expressed in spatially restricted domains of the forebrain, face and limbs in midgestation mouse embryos. Mech Dev. 1993a; 40:129–140. [PubMed: 8098616]

Bulfone A, Puelles L, Porteus MH, Frohman MA, Martin GR, Rubenstein JL. Spatially restricted expression of Dlx-1, Dlx-2 (Tes-1), Gbx-2, and Wnt-3 in the embryonic day 12.5 mouse forebrain defines potential transverse and longitudinal segmental boundaries. J Neurosci. 1993b; 13:3155–3172. [PubMed: 7687285]

Cobos I, Calcagnotto ME, Vilaythong AJ, Thwin MT, Noebels JL, Baraban SC, Rubenstein JL. Mice lacking Dlx1 show subtype-specific loss of interneurons, reduced inhibition and epilepsy. Nat Neurosci. 2005; 8:1059–1068. [PubMed: 16007083]

Cobos I, Borello U, Rubenstein JL. Dlx transcription factors promote migration through repression of axon and dendrite growth. Neuron. 2007; 54:873–888. [PubMed: 17582329]

Depew MJ, Liu JK, Long JE, Presley R, Meneses JJ, Pedersen RA, Rubenstein JL. Dlx5 regulates regional development of the branchial arches and sensory capsules. Development. 1999; 126:3831–3846. [PubMed: 10433912]

Depew MJ, Lufkin T, Rubenstein JL. Specification of jaw subdivisions by Dlx genes. Science. 2002; 298:381–385. [PubMed: 12193642]

Depew MJ, Simpson CA, Morasso M, Rubenstein JL. Reassessing the Dlx code: the genetic regulation of branchial arch skeletal pattern and development. J Anat. 2005; 207:501–561. [PubMed: 16313391]

Eisenstat DD, Liu JK, Mione M, Zhong W, Yu G, Anderson SA, Ghattas I, Puelles L, Rubenstein JL. DLX-1, DLX-2, and DLX-5 expression define distinct stages of basal forebrain differentiation. J Comp Neurol. 1999; 414:217–237. [PubMed: 10516593]

Faedo A, Quinn JC, Stoney P, Long JE, Dye C, Zollo M, Rubenstein JL, Price DJ, Bulfone A. Identification and characterization of a novel transcript down-regulated in Dlx1/Dlx2 and up-regulated in Pax6 mutant telencephalon. Dev Dyn. 2004; 231:614–620. [PubMed: 15376329]

Feng J, Bi C, Clark BS, Mady R, Shah P, Kohtz JD. The Evf-2 noncoding RNA is transcribed from the Dlx-5/6 ultra-conserved region and functions as a Dlx-2 transcriptional coactivator. Genes Dev. 2006; 20:1470–1484. [PubMed: 16705037]

Fischer AJ, Stanke JJ, Aloisio G, Hoy H, Stell WK. Heterogeneity of horizontal cells in the chicken retina. J Comp Neurol. 2007; 500:1154–1171. [PubMed: 17183536]

Jacobowitz, DM.; Abbott, LC. Chemoarchitectonic atlas of the developing mouse brain. Boca Raton: CRC Press; 1998.

Jeong J, Li X, McEvilly RJ, Rosenfeld MG, Lufkin T, Rubenstein JL. Dlx genes pattern mammalian jaw primordium by regulating both lower jaw-specific and upper jaw-specific genetic programs. Development. 2008; 135:2905–2916. [PubMed: 18697905]

Kim JH, Lee JA, Song YM, Park CH, Hwang SJ, Kim YS, Kaang BK, Son H. Overexpression of calbindin-D28K in hippocampal progenitor cells increases neuronal differentiation and neurite outgrowth. FASEB J. 2006; 20:109–111. [PubMed: 16278289]

Levi G, Puche AC, Mantero S, Barbieri O, Trombino S, Paleari L, Egeo A, Merlo GR. The Dlx5 homeodomain gene is essential for olfactory development and connectivity in the mouse. Mol Cell Neurosci. 2003; 22:530–543. [PubMed: 12727448]

Liu JK, Ghattas I, Liu S, Chen S, Rubenstein JL. Dlx genes encode DNA-binding proteins that are expressed in an overlapping and sequential pattern during basal ganglia differentiation. Dev Dyn. 1997; 210:498–512. [PubMed: 9415433]

Lobo MK, Karsten SL, Gray M, Geschwind DH, Yang XW. FACS-array profiling of striatal projection neuron subtypes in juvenile and adult mouse brains. Nat Neurosci. 2006; 9:443–452. [PubMed: 16491081]

Long JE, Garel S, Depew MJ, Tobet S, Rubenstein JL. DLX5 regulates development of peripheral and central components of the olfactory system. J Neurosci. 2003; 23:568–578. [PubMed: 12533617]

Long JE, Garel S, Alvarez-Dolado M, Yoshikawa K, Osumi N, Alvarez-Buylla A, Rubenstein JL. Dlx-dependent and -independent regulation of olfactory bulb interneuron differentiation. J Neurosci. 2007; 27:3230–3243. [PubMed: 17376983]

Long JE, Cobos I, Potter GB, Rubenstein JL. Dlx1&2 and Mash1 transcription factors control MGE and CGE patterning and differentiation through parallel and overlapping pathways. Cereb Cortex. 2009a; 19(suppl 1):i96–106. [PubMed: 19386638]

Long JE, Swan C, Liang WS, Cobos I, Potter GB, Rubenstein JL. Dlx1&2 and Mash1 transcription factors control striatal patterning and differentiation through parallel and overlapping pathways. J Comp Neurol. 2009b; 512:556–572. [PubMed: 19030180]

Mao R, Page DT, Merzlyak I, Kim C, Tecott LH, Janak PH, Rubenstein JL, Sur M. Reduced conditioned fear response in mice that lack Dlx1 and show subtype-specific loss of interneurons. J Neurodev Disord. 2009; 1:224–236. [PubMed: 19816534]

Marín O, Anderson SA, Rubenstein JL. Origin and molecular specification of striatal interneurons. J Neurosci. 2000; 20:6063–6076. [PubMed: 10934256]

Panganiban G, Rubenstein JL. Developmental functions of the Distal-less/Dlx homeobox genes. Development. 2002; 129:4371–4386. [PubMed: 12223397]

Pardo R, Colin E, Regulier E, Aebischer P, Deglon N, Humbert S, Saudou F. Inhibition of calcineurin by FK506 protects against polyglutamine-huntingtin toxicity through an increase of huntingtin phosphorylation at S421. J Neurosci. 2006; 26:1635–1645. [PubMed: 16452687]

Parras CM, Galli R, Britz O, Soares S, Galichet C, Battiste J, Johnson JE, Nakafuku M, Vescovi A, Guillemot F. Mash1 specifies neurons and oligodendrocytes in the post-natal brain. EMBO J. 2004; 23:4495–4505. [PubMed: 15496983]

Perera M, Merlo GR, Verardo S, Paleari L, Corte G, Levi G. Defective neuronogenesis in the absence of Dlx5. Mol Cell Neurosci. 2004; 25:153–161. [PubMed: 14962748]

Petryniak MA, Potter GB, Rowitch DH, Rubenstein JL. Dlx1 and Dlx2 control neuronal versus oligodendroglial cell fate acquisition in the developing forebrain. Neuron. 2007; 55:417–433. [PubMed: 17678855]

Pleasure SJ, Anderson S, Hevner R, Bagri A, Marín O, Lowenstein DH, Rubenstein JL. Cell migration from the ganglionic eminences is required for the development of hippocampal GABAergic interneurons. Neuron. 2000; 28:727–740. [PubMed: 11163262]

Porteus MH, Bulfone A, Liu JK, Puelles L, Lo LC, Rubenstein JL. DLX-2, MASH-1, and MAP-2 expression and bromodeoxyuridine incorporation define molecularly distinct cell populations in the embryonic mouse forebrain. J Neurosci. 1994; 14:6370–6383. [PubMed: 7965042]

Puelles L, Rubenstein JL. Forebrain gene expression domains and the evolving prosomeric model. Trends Neurosci. 2003; 26:469–476. [PubMed: 12948657]

Qiu M, Bulfone A, Martinez S, Meneses JJ, Shimamura K, Pedersen RA, Rubenstein JL. Null mutation of Dlx-2 results in abnormal morphogenesis of proximal first and second branchial arch derivatives and abnormal differentiation in the forebrain. Genes Dev. 1995; 9:2523–2538. [PubMed: 7590232]

Qiu M, Bulfone A, Ghattas I, Meneses JJ, Christensen L, Sharpe PT, Presley R, Pedersen RA, Rubenstein JL. Role of the Dlx homeobox genes in proximodistal patterning of the branchial arches: mutations of Dlx-1, Dlx-2, and Dlx-1 and -2 alter morphogenesis of proximal skeletal and soft tissue structures derived from the first and second arches. Dev Biol. 1997; 185:165–184. [PubMed: 9187081]

Regad T, Bellodi C, Nicotera P, Salomoni P. The tumor suppressor Pml regulates cell fate in the developing neocortex. Nat Neurosci. 2009; 12:132–140. [PubMed: 19136970]

Robledo RF, Rajan L, Li X, Lufkin T. The Dlx5 and Dlx6 homeobox genes are essential for craniofacial, axial, and appendicular skeletal development. Genes Dev. 2002; 16:1089–1101. [PubMed: 12000792]

Schiffmann SN, Cheron G, Lohof A, d'Alcantara P, Meyer M, Parmentier M, Schurmans S. Impaired motor coordination and Purkinje cell excitability in mice lacking calretinin. Proc Natl Acad Sci U S A. 1999; 96:5257–5262. [PubMed: 10220453]

Schwaller B, Buchwald P, Blumcke I, Celio MR, Hunziker W. Characterization of a polyclonal antiserum against the purified human recombinant calcium binding protein calretinin. Cell Calcium. 1993; 14:639–648. [PubMed: 8242719]

Senawong T, Peterson VJ, Avram D, Shepherd DM, Frye RA, Minucci S, Leid M. Involvement of the histone deacetylase SIRT1 in chicken ovalbumin upstream promoter transcription factor (COUP-TF)-interacting protein 2-mediated transcriptional repression. J Biol Chem. 2003; 278:43041–43050. [PubMed: 12930829]

Stühmer T, Anderson SA, Ekker M, Rubenstein JL. Ectopic expression of the Dlx genes induces glutamic acid decarboxylase and Dlx expression. Development. 2002a; 129:245–252. [PubMed: 11782417]

Stühmer T, Puelles L, Ekker M, Rubenstein JL. Expression from a Dlx gene enhancer marks adult mouse cortical GABAergic neurons. Cereb Cortex. 2002b; 12:75–85. [PubMed: 11734534]

Wang B, Waclaw RR, Allen ZJ 2nd, Guillemot F, Campbell K. Ascl1 is a required downstream effector of Gsx gene function in the embryonic mouse telencephalon. Neural Dev. 2009; 4:5. [PubMed: 19208224]

Wang Y, Dye C, Sohal V, Long J, Estrada R, Roztocil T, Lufkin T, Deisseroth K, Baraban S, Rubenstein JLR. Dlx5 and Dlx6 regulate the development of parvalbumin-expressing cortical interneurons. J Neurosci. 2010; 30:5334–45. [PubMed: 20392955]

Yee CL, Wang Y, Anderson S, Ekker M, Rubenstein JL. Arcuate nucleus expression of NKX2.1 and DLX and lineages expressing these transcription factors in neuropeptide Y(+), proopiomelanocortin(+), and tyrosine hydroxylase(+) neurons in neonatal and adult mice. J Comp Neurol. 2009; 517:37–50. [PubMed: 19711380]

Yun K, Fischman S, Johnson J, Hrabe de Angelis M, Weinmaster G, Rubenstein JL. Modulation of the notch signaling by Mash1 and Dlx1/2 regulates sequential specification and differentiation of progenitor cell types in the subcortical telencephalon. Development. 2002; 129:5029–5040. [PubMed: 12397111]

Zhao Y, Flandin P, Long JE, Cuesta MD, Westphal H, Rubenstein JL. Distinct molecular pathways for development of telencephalic interneuron subtypes revealed through analysis of Lhx6 mutants. J Comp Neurol. 2008; 510:79–99. [PubMed: 18613121]

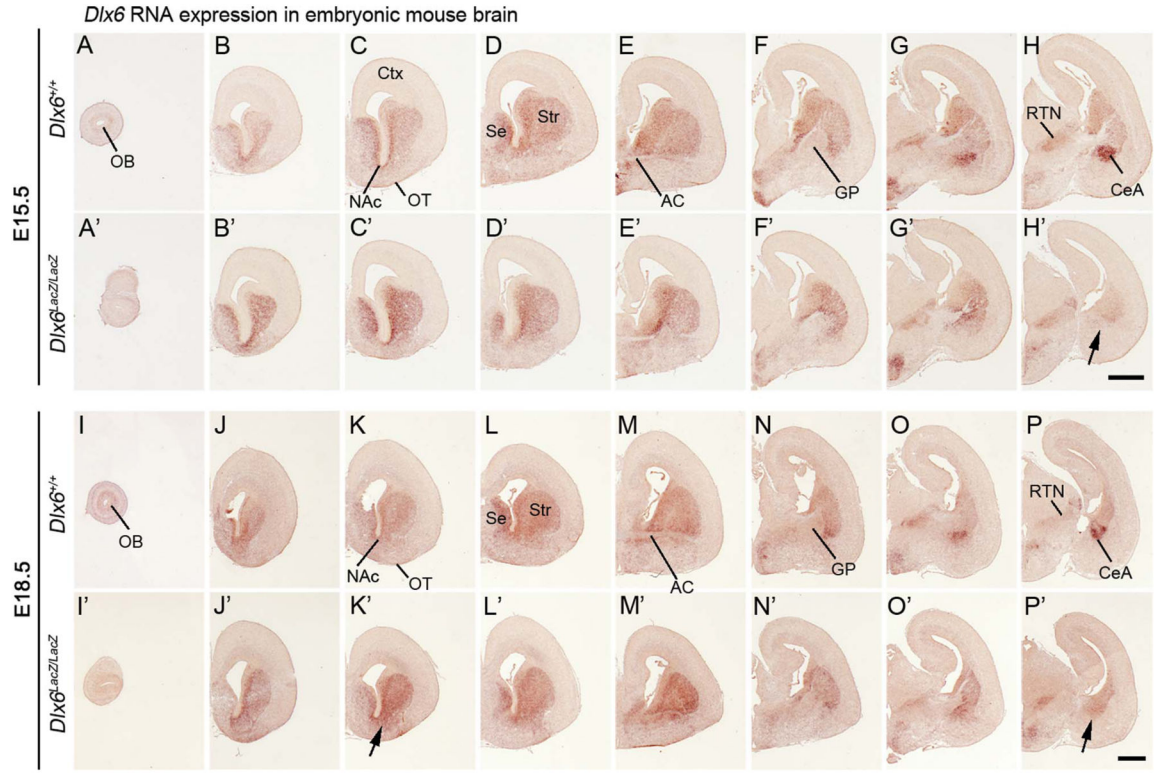

Figure 1.

A–P, A′–P′: *Dlx6* RNA expression in the wild-type and $Dlx6^{LacZ/LacZ}$ E15.5 and E18.5 forebrain; coronal hemisections are shown. Arrows point to regions of the telencephalon (CeA, NAc, and OT) where the $Dlx6^{LacZ/LacZ}$ mutant shows alterations in *Dlx6* RNA expression. Abbreviations: AC, anterior commissure; CeA, central nucleus of the amygdala; Ctx, neocortex; GP, globus pallidus; NAc, nucleus accumbens; OB, olfactory bulb; OT, olfactory tubercle; RTN, reticular nucleus of the thalamus; Se, septum; Str, striatum. Scale bar equals; 200 μm in P′ (applies to all). [Color figure can be viewed in the online issue, which is available at wileyonlinelibrary.com.]

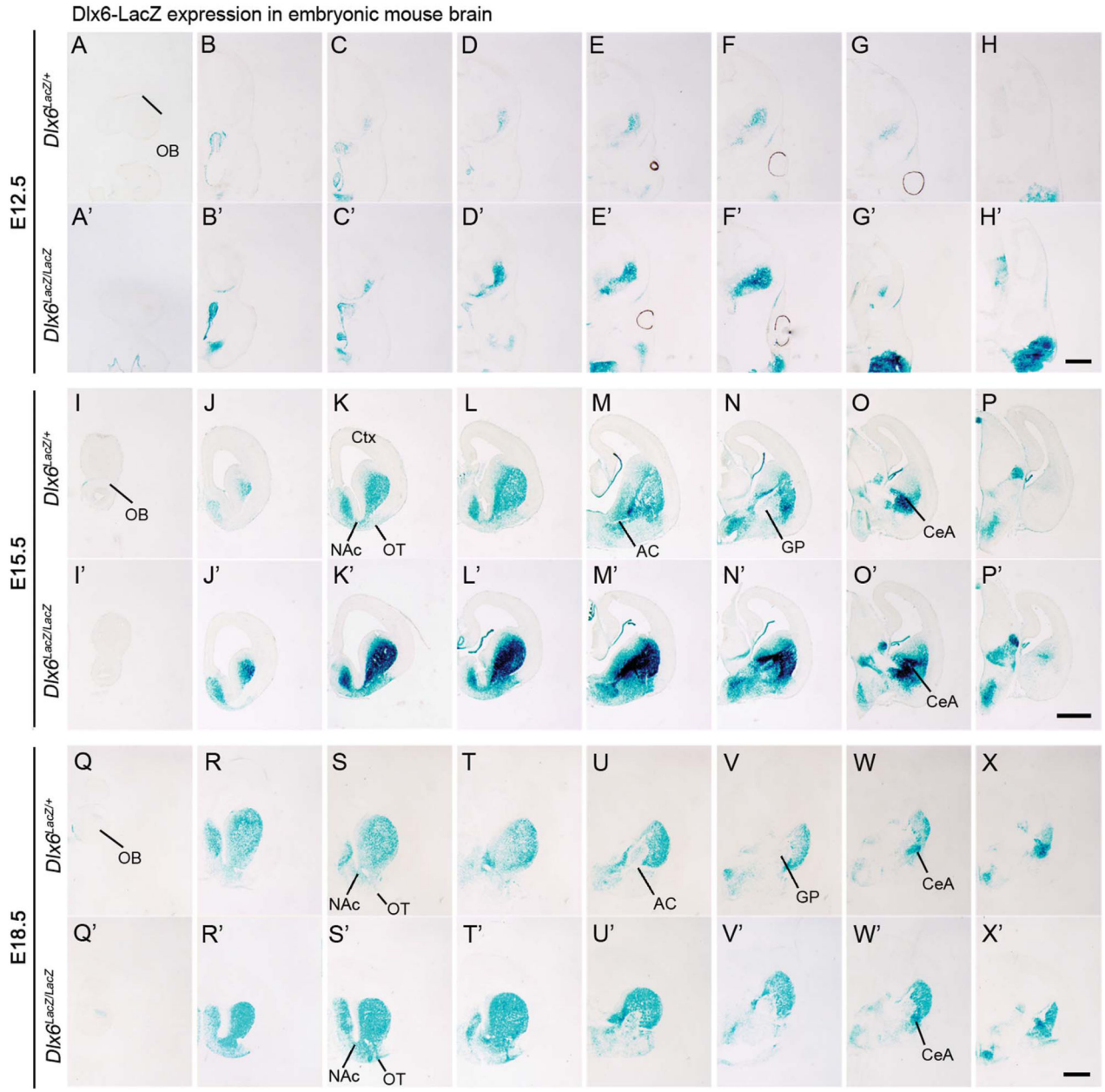

Figure 2.

A–X, A′–X′: β-Galactosidase expression in *Dlx6*$^{LacZ/+}$ and *Dlx6*$^{LacZ/LacZ}$ mice at E12.5, E15.5, and E18.5 shown in a rostrocaudal series of coronal hemisections. Abbreviations: AC, anterior commissure; CeA, central nucleus of the amygdala; Ctx, neocortex; GP, globus pallidus; NAc, nucleus accumbens; OB, olfactory bulb; OT, olfactory tubercle; RTN, reticular nucleus of the thalamus; Se, septum; Str, striatum. Scale bar equals; 100 μm in H′ (applies to A–H′); 200 μm in P′ (applies to I–P′); 200 μm in X′ (applies to Q–X′). [Color figure can be viewed in the online issue, which is available at wileyonlinelibrary.com.]

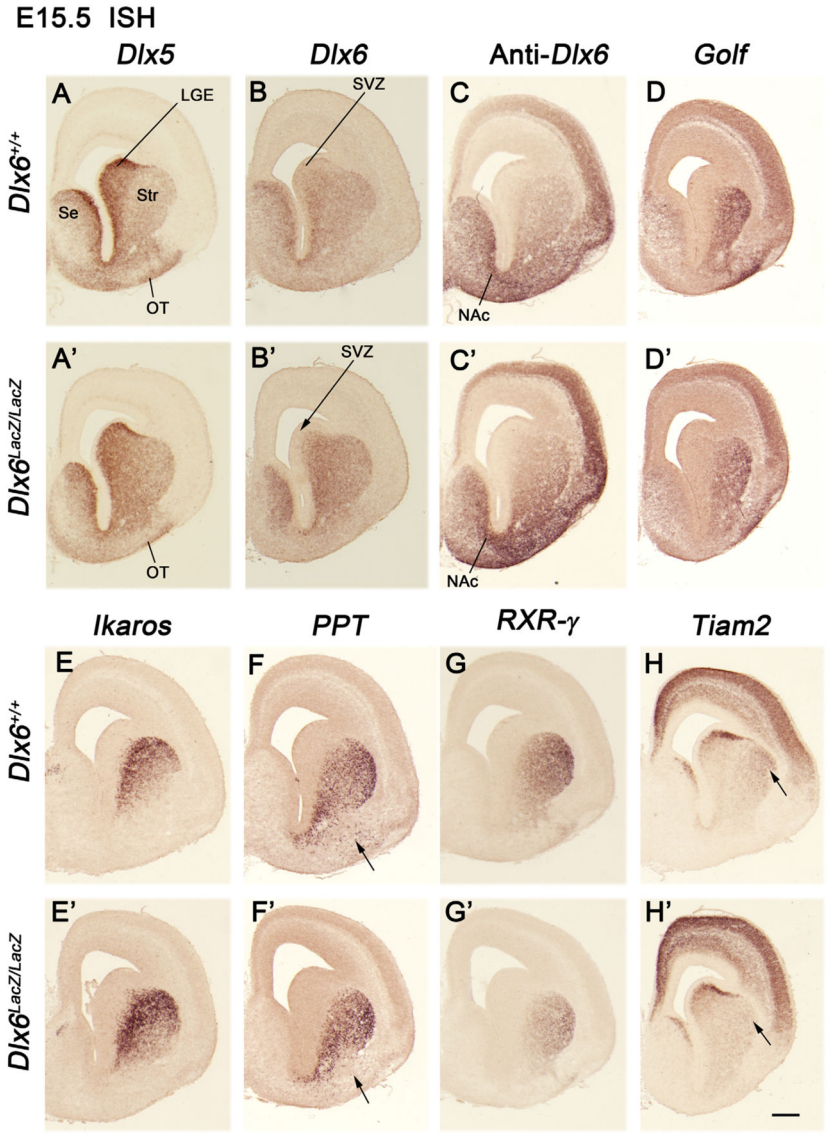

Figure 3.

A–H, A′–H′: Changes in the RNA expression of LGE and striatal markers at E15.5 in wild-type (*Dlx6*$^{+/+}$) and *Dlx6*$^{LacZ/LacZ}$ mice. In situ hybridization analysis of the rostral telencephalon; coronal hemisections are shown. The gene names are listed above the panels. Arrows point to regions of the telencephalon where the *Dlx6*$^{LacZ/LacZ}$ mutant shows alterations in *Dlx6* RNA expression. Abbreviations: LGE, lateral ganglionic eminence; NAc, nucleus accumbens; OT, olfactory tubercle; Se, septum; Str, striatum; SVZ, subventricular zone. Scale bar equals; 500 μm in H′ (applies to all). [Color figure can be viewed in the online issue, which is available at wileyonlinelibrary.com.]

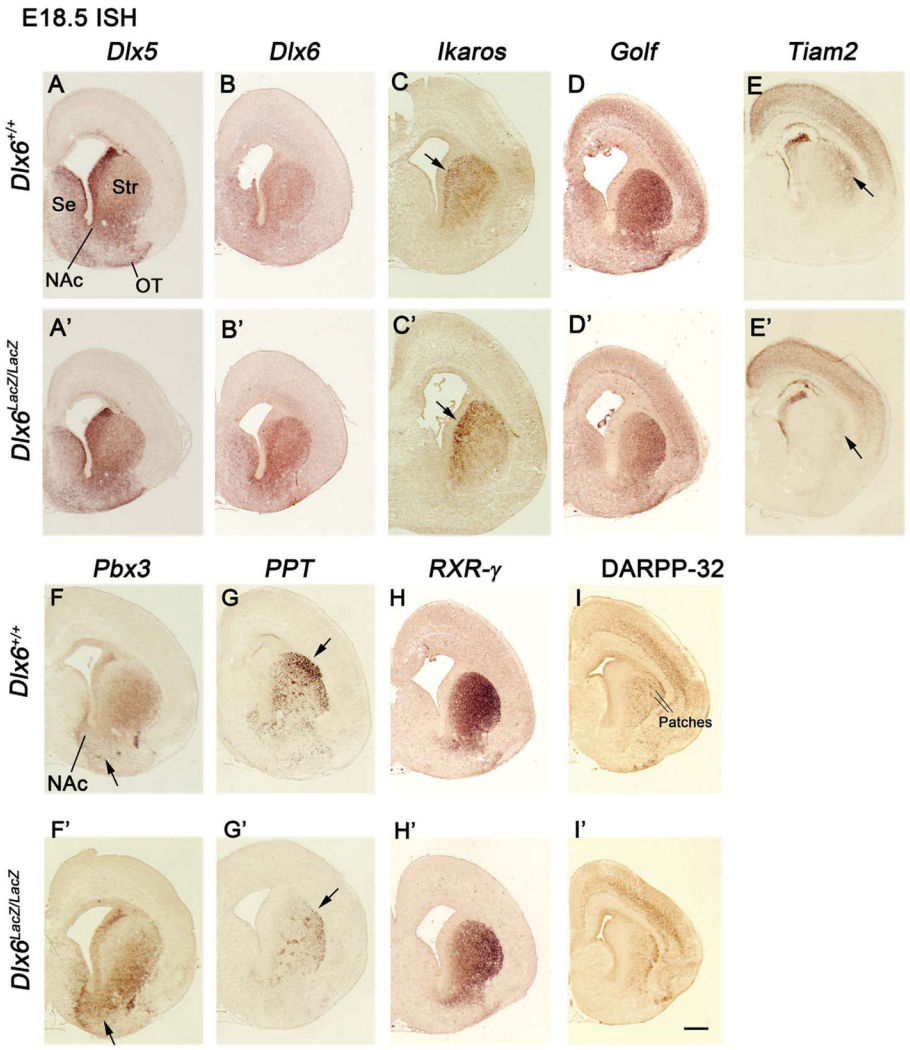

Figure 4.

A–I, A′–I′: Changes in the RNA expression of LGE and striatal markers at E18.5 in wild-type and *Dlx6*$^{LacZ/LacZ}$ mice. In situ hybridization and immunohistochemistry (I, I′) analysis of the rostral telencephalon; coronal hemisections are shown. The gene names are listed above the panels. Arrows point to regions of the telencephalon where the *Dlx6*$^{LacZ/LacZ}$ mutant shows alterations in *Dlx6* RNA expression. Abbreviations: NAc, nucleus accumbens; OT, olfactory tubercle; Se, septum; Str, striatum. Scale bar equals; 500 μm in I′ (applies to all). [Color figure can be viewed in the online issue, which is available at wileyonlinelibrary.com.]

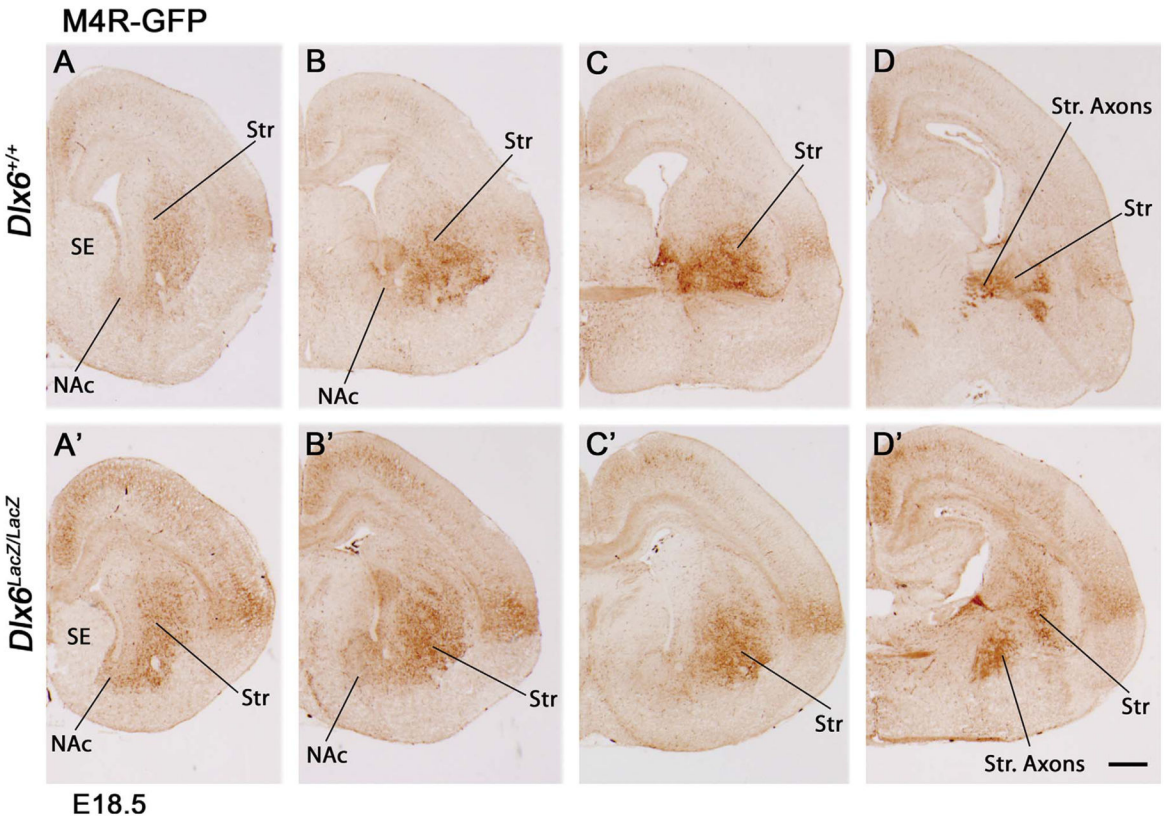

Figure 5.

A–D, A′–D′: Changes in the expression of M4R-GFP at E18.5 in coronal hemisections of wild-type and *Dlx6*$^{LacZ/LacZ}$ mice. The mutant shows increased expression of green fluorescent protein (GFP; immunohistochemistry) in the NAc. Abbreviations: NAc, nucleus accumbens; OT, olfactory tubercle; SE, septum; Str, striatum. Scale bar equals; 500 μm in D′ (applies to all). [Color figure can be viewed in the online issue, which is available at wileyonlinelibrary.com.]

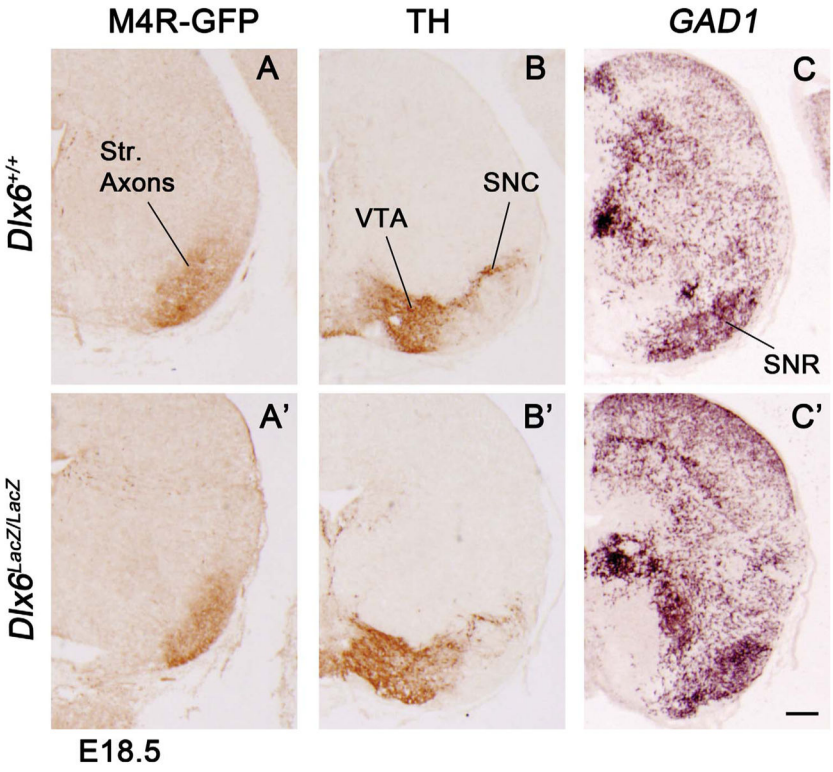

Figure 6.

A–C, A′–C′: M4R-GFP^{+} striatal projections at E18.5 to the substania nigra are intact in *Dlx6*$^{LacZ/LacZ}$. Coronal hemisections showing expression of GFP in striatal axons (immunohistochemistry), tyrosine hydroxylase (TH; immunohistochemistry) in the substantia nigra pars compacta (SNC) and the ventral tegmental area (VTA) and glutamic acid decarboxylase 1 (GAD1; in situ RNA hybridization) in the substantia nigra pars reticulata (SNR), and other midbrain regions. Scale bar equals; 500 μm in C′ (applies to all) [Color figure can be viewed in the online issue, which is available at wileyonlinelibrary.com.].

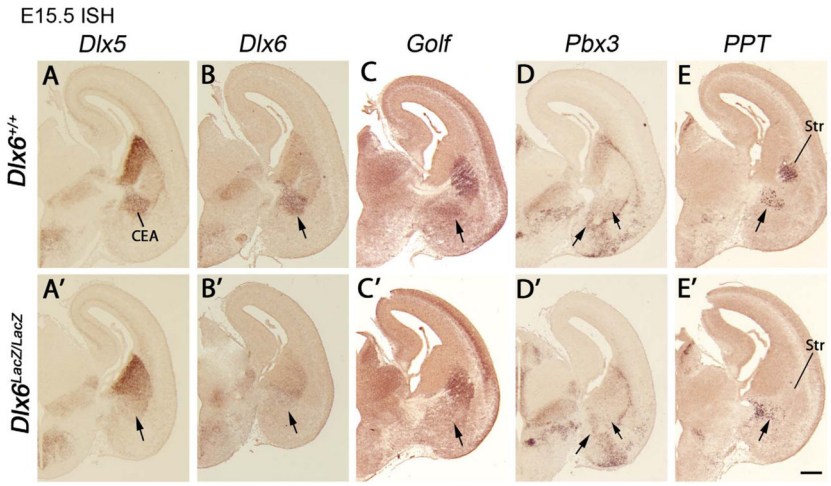

Figure 7.

A–E, A′–E′: Changes in expression of central nucleus of the amygdala (CeA) markers at E15.5 in wild-type and *Dlx6*$^{LacZ/LacZ}$ mice. In situ hybridization analysis of the caudal telencephalon; coronal hemisections are shown. The gene names are listed above the panels. Abbreviations: CeA, central nucleus of the amygdale; Str, striatum. Scale bar equals; 500 μm in E′ (applies to all). [Color figure can be viewed in the online issue, which is available at wileyonlinelibrary.com.]

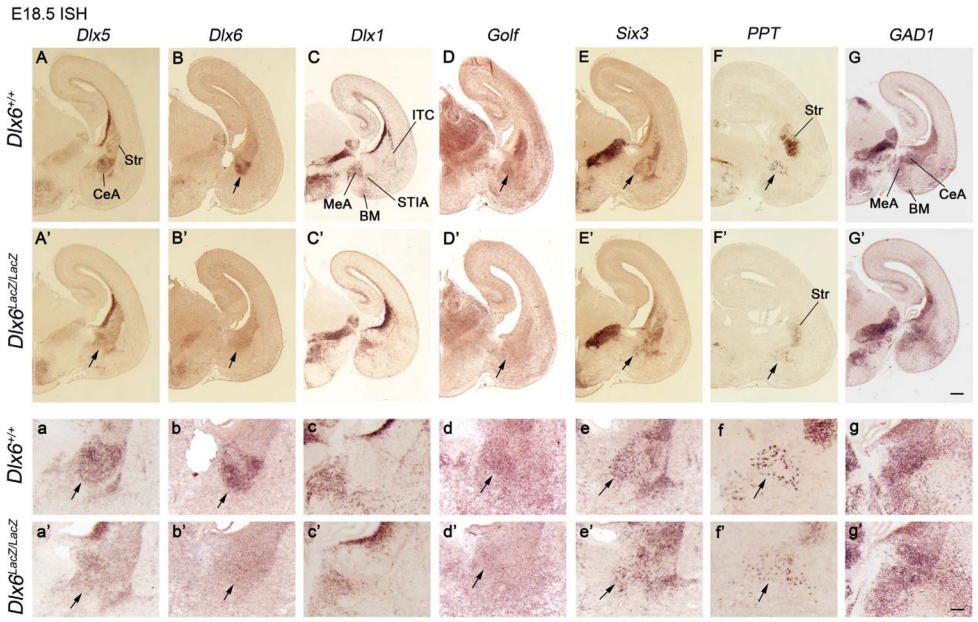

Figure 8.

Changes in expression of central nucleus of the amygdala (CeA) markers at E18.5 in wild-type and *Dlx6*$^{LacZ/LacZ}$ mice. **A–G′**: In situ hybridization analysis of the caudal telencephalon; coronal hemisections are shown. The gene names are listed above the panels. **a–g′**: Higher magnification views of the region of the CeA taken from the lower magnification photos above. Arrows point to regions where the *Dlx6*$^{LacZ/LacZ}$ mutant shows alterations in gene expression. Abbreviations: BM, basomedial nucleus; CeA, central nucleus of the amygdala; ITC, intercalated nucleus; MeA, medial nucleus of the amygdala; STIA, stria terminalis intraamygdaloid nucleus; Str, striatum. Scale bar equals; 500 μm in G′ (applies to A–G′); 200 μm in g′ (applies to a–g′). [Color figure can be viewed in the online issue, which is available at wileyonlinelibrary.com.]

TABLE 1

Antibody Reagents Used in This Study[1]

Antibody	Antigen	Species	Dilution	Source and cat. no.
Calbindin D-28K	Recombinant rat calretinin D-28k full length	Rabbit	1:4000	Swant, CB-38a
Calretinin	Recombinant human calretinin full length	Rabbit	1:2000	Swant, 7699/4
CITP2 (25B6)	Recombinant human CTIP2 full length. The epitope was mapped to between amino acids 1 and 150 of CTIP2.	Rat	1:1,000	Abcam, AB18465
DARPP32	Synthetic peptide (CQVEMIRRRRPTPAM) coupled to KLH	Rabbit	1:500	Chemicon, AB1656
Foxp1	Synthetic peptide (HDRDYEDEPVNEDME) conjugated to KLH derived from amino acids 663–677 of human FOXP1	Rabbit	1:200	Abcam, AB16645
GFP	GFP isolated directly from *Aequorea victoria*	Rabbit	1:1,000	Invitrogen, A11122
Phospho-histone H3	KLH-conjugated peptide (ARK(pS)TGGKAPRKQLC) corresponding to amino acids 7–20 of human histone H3	Rabbit	1:200	Cell Signaling, 9706

[1] Details on the specificity controls are described in Materials and Methods.

TABLE 2

Nucleotide Sequences of *In Situ* Hybridization Probes

Plasmid name	Source	Insert size (bp)	Beginning location NT from 3′ or primers used to generate
Brn4	Bryan Crenshaw	573	513–1,086
Cad8	Chris Redies	460	1,251–1,711
D1R	Josh Corbin	534	3,604–4,138
D2R	Josh Corbin	804	517–1,321
Dlx1	John Rubenstein	2,800	2,800 from 3′ end
Dlx2	John Rubenstein	1,700	1,700 from 3′ end
Dlx5	John Rubenstein	1,600	1,600 from 3′ end
Dlx6	John Rubenstein	210	210 from 3′ end; complementary to antisense strand
Anti-Dlx6	John Rubenstein	1,000	1,000 from 3′ end; complementary to sense strand
Ebf1	R. Grosschedl	737	193–930
Egr3	J.D. Powell	1,416	Full coding sequence
Enk	Josh Corbin	1,441	Full coding sequence
GAD67	Bryan Condie	2,000	Full coding sequence
Gbx1	Mike Frohman	550	334–884
Golf; Gna1	Richard Axel	1,540	1–1,540
Gucy1a3	ATCC 9841394	2,000	Full coding sequence
Ikaros	Katia Georgopoulos	1,093	243–1,336
Islet1	Tom Jessell	1,510	31–1,541
Lhx6	Vassilis Pachnis	1,342	1,208–2,550
Lmo4	Gordon Gill	500	Full coding sequence
Meis1	Kenneth Campbell	2,300	Full coding sequence
Meis2	Kenneth Campbell	2,400	Full coding sequence
Pbx1	Heike Pöpperl	1,294	358–1,652
Pbx3	Heike Pöpperl	1,323	Full coding sequence
Preprotachykinin	Invitrogen	1,034	Image clone 1166182
Robo1	M. Tessier-Lavigne	1,000	1,000 from 3′ end
Robo2	M. Tessier-Lavigne	1,700	1,700 from 3′ end
RXRγ	Kenneth Campbell	1,226	907–2,133
Six3	Peter Gruss	650	650 from 3′ end
Sox1	R Lovell Badge	940	1,851–2,791
Tiam2	RZPD; ImaGenes	5,148	Full coding sequence